

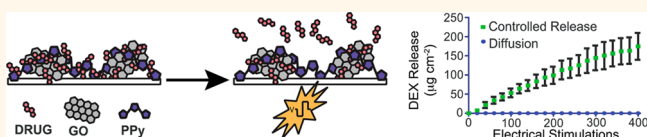


# Electrically Controlled Drug Delivery from Graphene Oxide Nanocomposite Films

Cassandra L. Weaver,<sup>†,‡,§</sup> Jaclyn M. LaRosa,<sup>†</sup> Xiliang Luo,<sup>⊥</sup> and Xinyan Tracy Cui<sup>†,‡,§,\*</sup>

<sup>†</sup>Department of Bioengineering, <sup>‡</sup>Center for the Neural Basis of Cognition, <sup>§</sup>McGowan Institute for Regenerative Medicine, University of Pittsburgh, Pittsburgh, Pennsylvania 15260, United States and <sup>⊥</sup>College of Chemistry and Molecular Engineering, Qingdao University of Science and Technology, Qingdao 266042, People's Republic of China

**ABSTRACT** On-demand, local delivery of drug molecules to target tissues provides a means for effective drug dosing while reducing the adverse effects of systemic drug delivery. This work explores an electrically controlled drug delivery nanocomposite composed of graphene oxide (GO) deposited inside a conducting polymer scaffold. The nanocomposite is loaded with an anti-inflammatory molecule, dexamethasone, and exhibits favorable electrical properties. In response to voltage stimulation, the nanocomposite releases drug with a linear release profile and a dosage that can be adjusted by altering the magnitude of stimulation. No drug passively diffuses from the composite in the absence of stimulation. *In vitro* cell culture experiments demonstrate that the released drug retains its bioactivity and that no toxic byproducts leach from the film during electrical stimulation. Decreasing the size and thickness of the GO nanosheets, by means of ultrasonication treatment prior to deposition into the nanocomposite, alters the film morphology, drug load, and release profile, creating an opportunity to fine-tune the properties of the drug delivery system to meet a variety of therapeutic needs. The high level of temporal control and dosage flexibility provided by the electrically controlled GO nanocomposite drug delivery platform make it an exciting candidate for on-demand drug delivery.



**KEYWORDS:** graphene oxide · conducting polymers · drug delivery · controlled release · nanocomposites

**O**n-demand release of drug molecules from biomedical devices enables precise, targeted dosing that can be temporally tuned to meet requirements for a variety of therapeutic applications.<sup>1–3</sup> Recent advances have facilitated the use of various cues, such as UV- and visible-wavelength light, NIR radiation, magnetic field, ultrasound and electrical stimulation to trigger drug release *in vivo* from implanted smart materials.<sup>1,4,5</sup> These techniques enable greater control over drug delivery, compared to traditional *in vivo* drug-release systems that rely on passive delivery that is programmed prior to implantation and cannot be modified in response to changing therapeutic needs. To achieve precise, controlled drug delivery, nanomaterial drug carriers are increasingly investigated because of their unique structures and tunable properties.<sup>6,7</sup> For example, the large surface area and  $sp^2$  carbon lattice associated with carbon nanomaterials, such as carbon nanotubes, graphene, and graphene oxide (GO), enable highly efficient drug loading, while their

capacity for modification provides multiple routes for targeted and controlled drug delivery.<sup>8,9</sup>

GO is a two-dimensional nanomaterial composed of a honeycomb carbon lattice structure with hydroxyl, carboxyl, and epoxide functional groups.<sup>10</sup> It is known for its exceptional electrical, chemical, and mechanical properties and has been investigated recently as a material for a variety of biomedical applications.<sup>9,11–15</sup> Of these applications, targeted drug delivery has been particularly interesting. The presence of reactive functional groups at the basal plane and edges of GO nanosheets creates an opportunity to covalently modify the particles for use in targeted drug delivery, while the abundance of localized  $\pi$ -electrons at the nanosheet surface enables  $\pi$ – $\pi$  interactions with aromatic drug compounds.<sup>16,17</sup> Targeted drug delivery has been achieved by covalently modifying drug-loaded GO with cancer-cell-targeting antibodies and molecules or by functionalization with paramagnetic particles for magnetically directed

\* Address correspondence to xic11@pitt.edu.

Received for review December 3, 2013 and accepted January 15, 2014.

Published online January 15, 2014  
10.1021/nn406223e

© 2014 American Chemical Society

delivery.<sup>18–22</sup> However, once at the targeted location, these methods rely on desorption of the drug molecules from the GO nanosheets through either passive or pH/redox-controlled mechanisms, which limits the ability to control the drug dosage in real time.<sup>17,20</sup> A drug-loaded hydrogel composed of reduced GO and poly(vinyl alcohol) enabled on-demand control of dosing *via* modulation of drug-release rate with the application of an external electric field.<sup>23</sup> However, this system required the use of large voltages that could be damaging to biological tissues, and drug passively diffused from the bulk of the polymer in the absence of stimulation because of the porous morphology of the hydrogel.

In this work, we describe an electrically controlled drug delivery system based on GO nanosheets incorporated into a conducting polymer (CP) film. CP-mediated drug delivery systems, composed of an electrode coated with a drug-loaded CP thin film, yield highly flexible release profiles that are favorable for addressing dosing needs that may change over the course of treatment.<sup>24</sup> Drug-loaded CP films release drug molecules in response to electrical stimulation, with the amount and duration of release controlled by the type of stimulation applied to the film.<sup>25–27</sup> A major limitation of CP-mediated drug release is the finite amount of drug that can be loaded into and released from the thin films. We address this shortcoming in CP-mediated release systems by developing a CP nanocomposite film composed of poly(pyrrole) (PPy) doped with GO nanosheets for controlled delivery of anti-inflammatory drugs.

Nanocomposite films consisting of GO nanosheets and CPs have recently generated interest as materials for bioapplications, such as cell scaffolding or chemical sensing, as a result of their favorable electrical properties, good stability, neuronal biocompatibility, and ease of surface modification with bioactive molecules.<sup>11,28–31</sup> We demonstrate that, when incorporated into PPy along with the anti-inflammatory drug dexamethasone (DEX), the GO nanosheets create a highly stable

nanocomposite film that releases the drug molecules on-demand in response to electrical stimulation, without passive diffusion. The CP matrix provides a conductive scaffold through which electrical stimulation can be applied in order to elicit drug release from the nanocomposite, while the GO nanosheets act as nanocarriers that improve the amount of drug loaded into and released from the nanocomposite film. Furthermore, altering the thickness and size of the GO nanosheets by utilizing its unique response to sonication treatment changes the physical properties and release profile of the nanocomposite, suggesting that the system can be tuned to the needs of various applications, making it a valuable tool for both therapeutics and research within the field of biomedicine.

## RESULTS AND DISCUSSION

### GO/PPy Nanocomposite Film Synthesis and Characterization.

The DEX-loaded GO/PPy (GO/PPy-DEX) films were electrodeposited onto glassy carbon electrodes from a solution containing both GO nanosheets and DEX. During CP film polymerization, negatively charged species are loaded into the polymer matrix to balance positive charges formed on the backbone of the growing polymer. The GO nanosheets are negatively charged as a consequence of carboxylic acid groups formed at their edges during the oxidation procedure, enabling them to be incorporated into the CP film as dopant molecules, along with anionic drug molecules (Figure 1a). During the electropolymerization reaction, the GO nanosheets compete with the free anionic DEX, as dopant molecules. Fourier transform IR spectra of the GO/PPy-DEX film display peaks attributable to both GO and DEX, indicating that the drug molecules are successfully loaded into the film, along with the GO nanosheets (Supporting Information Figure S1). GO nanosheets have been noted for their large surface/volume ratio and  $sp^2$ -hybridized carbon structure, which enables efficient loading of aromatic drug molecules, such as DEX.<sup>9,32</sup> Therefore, although some DEX molecules are directly doped into the film, a portion of

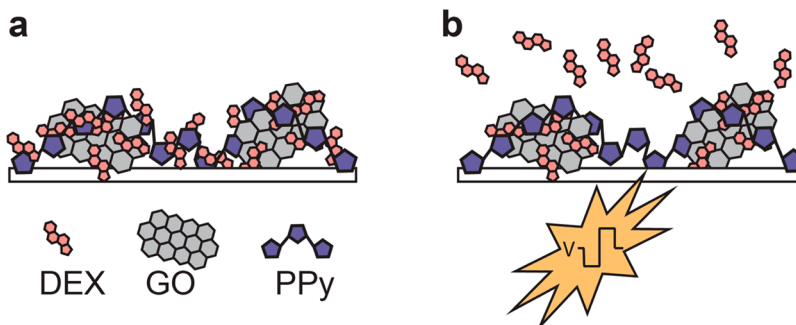


**Figure 1.** Drug loading into and release from the GO/PPy nanocomposite. Schematic representation of the (a) GO/PPy-DEX nanocomposite and (b) DEX release from the GO/PPy nanocomposite in response to electrical stimulation. During synthesis, positive charges form on the growing polymer backbone and are balanced by anions, such as GO and DEX molecules, present in the deposition solution. Reduction of the nanocomposite with voltage stimulation elicits release of small, mobile drug molecules as the polymer backbone neutralizes.

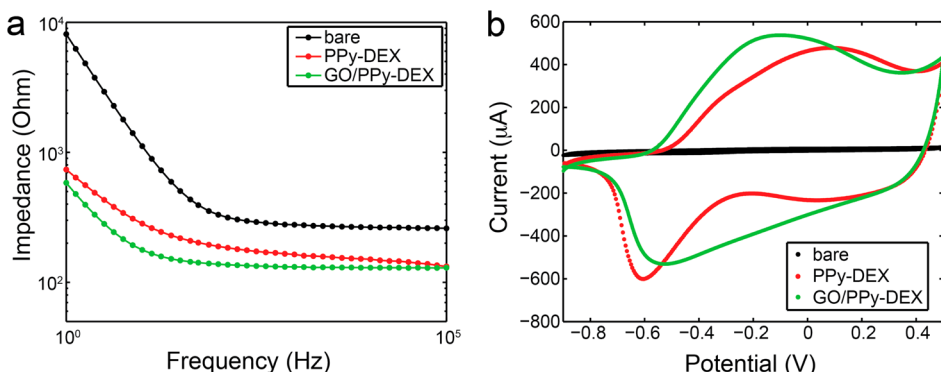


**Figure 2.** Electrical properties of the GO/PPy-DEX nanocomposite film. (a) Electrochemical impedance spectra and (b) cyclic voltammograms for bare glassy carbon electrodes, electrodes modified with a PPy-DEX film, and electrodes modified with the GO/PPy-DEX nanocomposite film. The GO/PPy-DEX-modified electrodes exhibit lower impedance values and higher charge-storage capacity, indicating the electroactivity of the nanocomposite.

the drug molecules may adsorb on the GO nanosheets and be carried into the synthesized composite films as the nanosheets are incorporated as dopant molecules.

The electrical properties of the GO/PPy-DEX film were explored using electrochemical impedance spectroscopy and cyclic voltammetry (CV) and compared to conventional PPy-DEX films that do not contain GO nanosheets as codopants. The electrode modified with GO/PPy-DEX film exhibited an impedance drop across all measured frequencies compared to both the bare electrode and the electrode modified with PPy-DEX, indicating that the nanocomposite film improves the capacitance of the electrode/electrolyte interface (Figure 2a). CV analysis carried out in phosphate buffered saline (PBS) showed that the electrodes modified with GO/PPy-DEX film have a higher charge-storage capacity, compared to both bare electrodes and PPy-DEX-modified electrodes, as determined by comparison of the area underneath the CV curves (Figure 2b). The CV curve of the GO/PPy-DEX-modified electrode exhibits a reduction peak at  $-0.52\text{ V}$  that occurs as anionic DEX molecules leave the film as a consequence of the negative potential sweep through the film and an oxidation peak at  $-0.09\text{ V}$  that is associated with redoping by small ions in the PBS or by DEX previously adsorbed on GO.<sup>33</sup> The GO/PPy-DEX reduction peak is much broader with a higher amount of current passed between  $0$  and  $-0.5\text{ V}$ . The larger reduction peak area, which reflects the amount of drug molecules leaving the film, suggests that the GO/PPy-DEX film will release drug more effectively than the PPy-DEX film. The low impedance and high charge-storage capacity of the synthesized nanocomposite reflect the excellent electrochemical properties of the nanocomposite film; as these properties decrease and increase, respectively, more current will pass through the film in response to a particular voltage pulse, enabling more efficient drug release.

**Electrically Controlled Drug Release from GO/PPy Nanocomposite Film.** Electrically controlled release of DEX molecules can be achieved by utilizing the unique

redox properties of the GO/PPy-DEX nanocomposite film. When the film is electrochemically reduced, the anionic DEX molecules previously associated with the positive charges along the PPy backbone in the oxidized form will be released as the charges on the polymer backbone are neutralized (Figure 1b). Since large dopant molecules are generally immobile within CP films, the GO nanosheets, which measure from hundreds of nanometers to micrometers in the  $x$ -/ $y$ -direction, are expected to remain within the CP during film reduction.<sup>10,33</sup> To evaluate the drug-releasing performance of the GO/PPy-DEX nanocomposite film, voltage pulses were applied through the nanocomposite when immersed in PBS, and the release solution was analyzed by UV absorbance spectroscopy to quantify the amount of DEX expelled from the film. Drug release from the GO/PPy-DEX nanocomposite was compared to release from conventional PPy-DEX films that do not contain GO nanosheets as codopants. The films were stimulated with an aggressive, biphasic voltage pulse ( $-2\text{ V}$  for  $5\text{ s}$ , followed by  $0\text{ V}$  for  $5\text{ s}$ ) for 1000 cycles to evaluate the total DEX release from the films (Figure 3a). When the PPy films were codoped with GO nanosheets, the aggressive release paradigm elicited  $2.3\times$  the amount of drug release of conventional PPy films without GO ( $209.7\text{ }\mu\text{g cm}^{-2}$  vs  $88.9\text{ }\mu\text{g cm}^{-2}$ ,  $p < 0.01$ ,  $n = 3$ ). Conducting polymer-mediated drug release is thought to be a surface-area-dependent process, with drug releasing more efficiently from the surface than the bulk of the film.<sup>27,34</sup> The nanocomposite film exhibits a much rougher surface morphology than conventional PPy films without GO (Supporting Information Figure S2), and the difference in the film surface area is a possible cause of the significant improvement in drug payload.

To determine the maximum amount of drug released from the GO/PPy-DEX nanocomposite film, the cumulative release profile in response to the aggressive stimulation was evaluated. After 600 stimulations, the drug-release profile reaches a plateau, suggesting that no more drug can be released from the

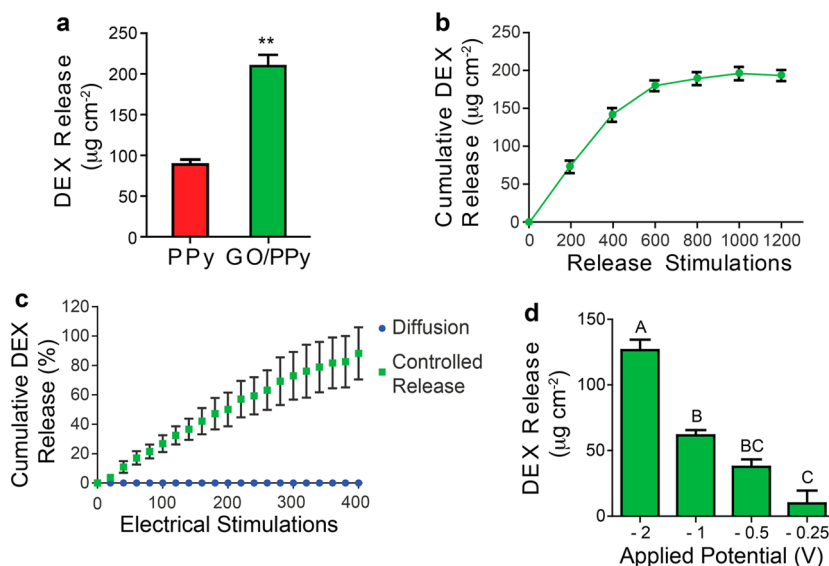


**Figure 3.** Electrically controlled DEX release from GO/PPy nanocomposite film. (a) Total DEX release from PPy films with or without GO as a codopant in response to an aggressive square wave, biphasic voltage stimulation ( $-2.0\text{ V}$  for 5 s, followed by  $0\text{ V}$  for 5 s) repeated for 1000 stimulations. The GO/PPy-DEX nanocomposite released a significantly larger quantity of DEX ( $p < 0.01$ ;  $n = 3$ ). (b) Cumulative release profile of the GO/PPy-DEX nanocomposite in response to aggressive repeated square wave, biphasic voltage stimulation ( $-2.0\text{ V}$  for 5 s, followed by  $0\text{ V}$  for 5 s) for 1200 stimulations ( $n = 6$ ). The release profile reaches a plateau at 600 voltage pulses under this aggressive stimulation paradigm, indicating that all available drug has been released at this point. (c) Cumulative release profile of the GO/PPy-DEX nanocomposite in response to milder release stimulation ( $-0.5\text{ V}$  for 5 s, followed by  $0.5\text{ V}$  for 5 s) and in the absence of electrical stimulation (passive diffusion) ( $n = 3$ ). Electrical stimulation elicited linear release for up to 400 pulses, while no drug passively diffused from the film when no voltage stimulation was applied. (d) Effect of voltage stimulus modulation on amount of DEX released from nanocomposite films. GO/PPy-DEX nanocomposite films were submitted to 100 square wave, biphasic stimulation pulses where the negative phase was varied from  $-2$  to  $-0.25\text{ V}$ , the positive phase was  $0.5\text{ V}$ , and the stimulus lingered at each phase for 5 s. Bars labeled with nonmatching letters indicate a significant difference between groups ( $p < 0.01$ ,  $n = 3$ ).

GO/PPy-DEX film (Figure 3b). Small quantities of DEX can be repeatedly released from the GO/PPy-DEX film in response to milder electrical stimulation ( $-0.5\text{ V}$  for 5 s, followed by  $0.5\text{ V}$  for 5 s), creating a drug-release profile that is linear over 400 stimulations, while no observable amount of drug passively diffuses from the film in the absence of stimulation (Figure 3c). Modulation of the voltage stimulation magnitude altered the amount of drug released from the nanocomposite, demonstrating the flexibility and high level of dosage control provided by the release system (Figure 3d). There was no visible cracking or delamination of the GO/PPy-DEX film after 1000 release stimulations ( $-0.5\text{ V}$  for 5 s, followed by  $0.5\text{ V}$  for 5 s), reflecting the good stability of the nanocomposite (Supporting Information Figure S3). The sustained linear release profile, responsiveness to changes in stimulation magnitude, and stability following repeated stimulation demonstrate the potential of the GO/PPy nanocomposite for applications requiring long-term and temporally precise drug dosing.

The bioactivity of the released drug was assessed by addition of solutions containing DEX released from GO/PPy films to primary astrocyte cultures and evaluation of the extent of interruption in cell proliferation. DEX is a synthetic glucocorticoid (GC) commonly used to treat inflammation and is used here as a model drug to demonstrate the efficacy of the released drug.

Chronic DEX exposure has been shown to interrupt astrocyte proliferation, likely by down-regulating GC receptor expression.<sup>35</sup> Astrocyte cultures exposed to the release solution or a prepared DEX solution ( $1\text{ }\mu\text{M}$ ) showed similar reductions in cell density after 4 days of culture, compared to control cultures that received no drug treatment (Figure 4,  $p < 0.05$ ). The drug-release solutions were obtained using the aggressive stimulation paradigm ( $-2\text{ V}$  for 5 s, followed by  $0\text{ V}$  for 5 s, 1000 cycles). These data indicate that the process of loading and stimulated release does not detectably alter the bioactivity of DEX molecules. However, it should be noted that, within the release solution, there are drug molecules that were released during early cycles as well as later cycles. Therefore, it is possible that if some of the drug released during the later cycles lost bioactivity as a result of repeated exposure to the voltage stimulation, the loss would be obscured by the presence of the more bioactive drug released by earlier cycles. Future work is needed to further elucidate the ability of DEX and other drug molecules to withstand chronic exposure to voltage stimulation while encapsulated in the nanocomposite film.

The safety of graphene nanoparticles for use in bio-applications has been questioned as a result of a growing body of evidence indicating the potential toxicity of soluble nanomaterials.<sup>12,36,37</sup> To exclude the possibility of potential release of any toxic byproducts

from the GO/PPy film, including soluble GO nanosheets, DEX release solutions were applied to primary neurons, a more sensitive cell population that does not proliferate and should be unresponsive to DEX treatment. In addition, GO/PPy films without drug loading underwent

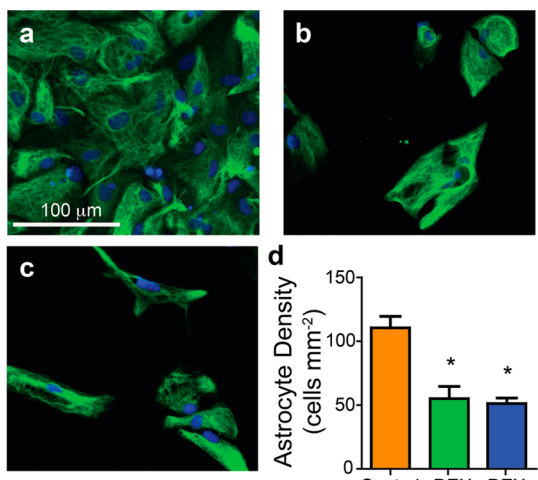


**Figure 4.** Bioactivity of DEX released from GO/PPy nanocomposite film. Representative fluorescent images of astrocyte cultures exposed to (a) no drug (control), (b) DEX released from GO/PPy nanocomposite films (rDEX), and (c) prepared solutions of  $1 \mu\text{M}$  DEX (DEX). GFAP (green); Hoechst 33342 (blue). (d) Density of astrocyte cultures 4 days after exposure to drug treatment. \*Indicates significant difference from control ( $p < 0.05$ ,  $n = 4$ ).

the same stimulation protocol as drug-loaded films, and the release solution was applied to neuron cultures. No effect on neuronal cell density was observed under either condition after 2 days of exposure (Figure 5), and the cells exhibited robust, interconnected neurite extensions indicative of healthy growth. This suggests that the interruption of astrocyte growth in response to the application of released DEX was due to specific actions of DEX, rather than nonspecific cytotoxicity from components of the GO/PPy film, such as monomer or GO nanosheets that may have delaminated from the electrode during electrical stimulation.

**Tuning of Nanocomposite Properties.** During chemical synthesis of GO, oxidized graphite sheets are commonly exfoliated with ultrasonication to obtain single- and few-layer GO (s/fGO) nanosheets. During sonication, the sheets also are reduced in the  $x$ - $y$ -dimension to create a smaller particle size that can measure as few as hundreds of nanometers, depending on the extent of sonication treatment.<sup>10,38</sup> To investigate the effect of altering the GO nanosheet size on the properties of the nanocomposite, GO suspensions were submitted to 30 or 60 min of sonication immediately prior to incorporation into the nanocomposite film. Atomic force microscopy measurements verified that the sonication treatment successfully reduced the size and thickness of the GO nanosheets. After 60 min of sonication, the distribution of nanosheet thickness shifted to smaller

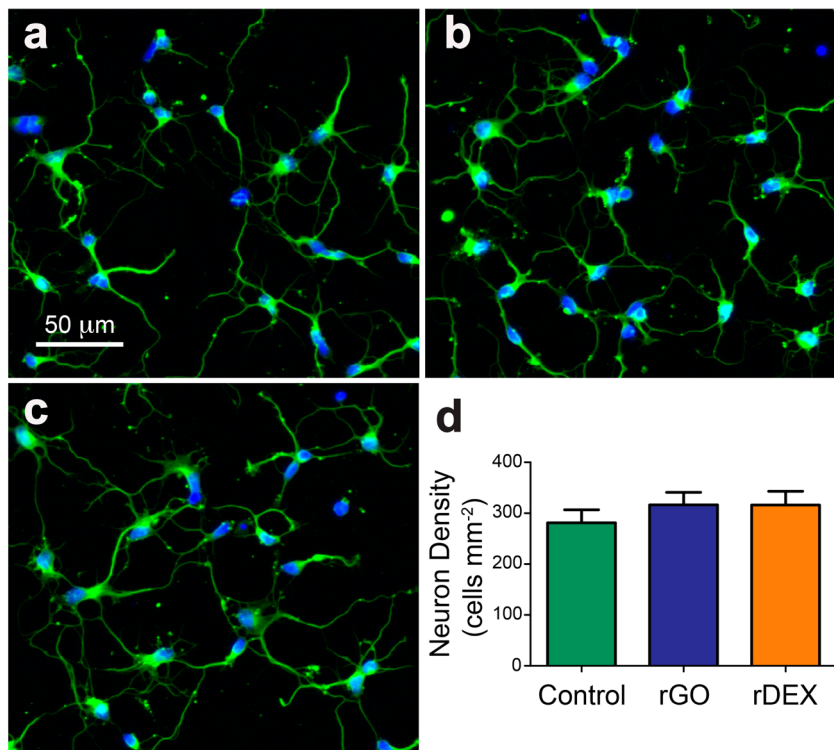


**Figure 5.** Effect of released DEX on neuronal cultures. Representative fluorescent images of neurons treated with (a) no drug (control), (b) release solutions from GO/PPy films without DEX loaded (rGO), or (c) release solutions from GO/PPy-DEX films (rDEX). Green,  $\beta$ -III-tubulin; blue, Hoechst 33342. (d) Neuronal density after 2 days of exposure to drug treatment. The treated cultures showed no significant difference, compared to control cultures ( $n = 4$ ).

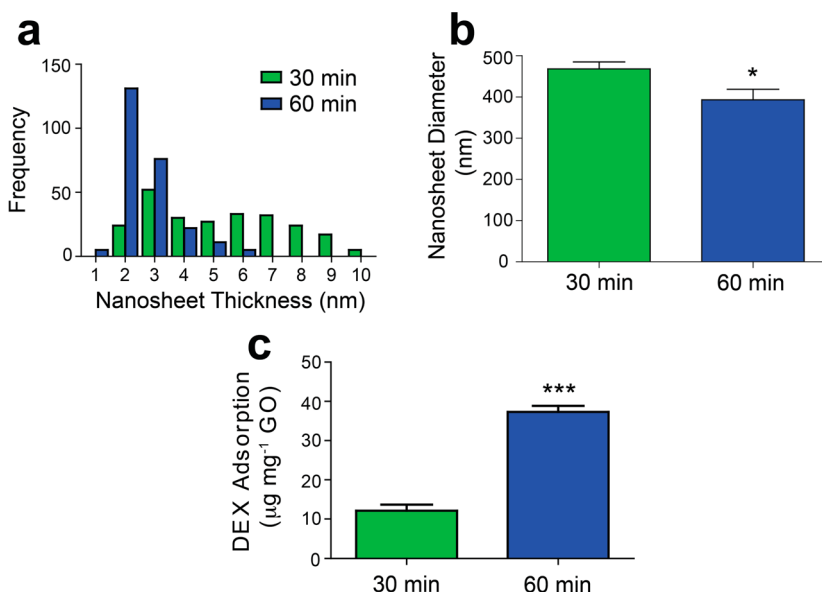


**Figure 6.** Effect of ultrasonication on GO nanosheet properties. (a) Histogram of nanosheet thickness and (b) average diameter of nanosheets after 30 and 60 min sonication (\* $p < 0.05$ ,  $n = 6$ ). (c) Amount of DEX adsorbed by free GO nanosheets (\*\* $p < 0.001$ ;  $n = 3$ ). Increasing duration of sonication treatment results in GO nanosheets that are thinner and smaller in diameter and that adsorb more DEX molecules.

values, compared to the distribution in the 30 min treatment group, indicating that the nanosheets were exfoliated into more s/fGO sheets (Figure 6a). As expected, the mean diameter of the GO nanosheets also decreased as the duration of sonication treatment increased (467.8 nm vs 392.7 nm,  $p < 0.05$ ), verifying that the mechanical vibrations created during sonication break the nanosheets into smaller pieces (Figure 6b). The size and thickness of the GO nanosheets can dictate their physiochemical properties, such as surface area, colloidal stability, and surface chemistry, all of which can affect the deposition and properties of the nanocomposite film.<sup>10,39</sup>

With longer sonication, the soluble GO nanosheets physically adsorb a larger amount of DEX molecules per unit mass (Figure 6c). The increase in loading capacity likely stems from the larger amount of GO surface area that is created within the suspension as multilayer GO nanosheets are exfoliated into multiple s/fGO particles. The propensity of graphene and GO to adsorb drug molecules such as DEX arises from the abundance of 2p orbitals extending from the planar surface of the nanomaterial that will readily participate in  $\pi-\pi$  interactions with aromatic compounds.<sup>10,17</sup> Therefore, it is expected that, as surface area increases through exfoliation, more active locations are uncovered, and a larger quantity of drug molecules may be adsorbed. The improved loading capacity of GO may enable the nanomaterial to act as a nanocarrier by shuttling adsorbed drug into the nanocomposite film and increasing the total drug load. The extent to which GO sonication treatment affects drug load into the nanocomposite was evaluated by elemental analysis using energy-dispersive spectroscopy (EDS). EDS of the

DEX-loaded nanocomposite films provided a semi-quantitative summary of the amount of drug loaded into the film. Each DEX molecule contains one fluorine atom, and each subunit of PPy contains one nitrogen atom. Thus, the ratio of fluorine atoms to nitrogen atoms in the film corresponds to the amount of drug loading. As expected, nanocomposite films synthesized with GO sonicated for 60 min loaded more drug than those in the 30 min sonication group, as indicated by the F/N ratio (Figure 7a,  $p < 0.01$ ). Interestingly, although increased GO sonication led to higher drug loading into the nanocomposite, the rate of DEX released from the film in response to voltage pulse stimulation was 38% higher for the nanocomposite synthesized with GO sonicated for 30 min, compared to the 60 min sonication group (Figure 7b,  $p < 0.05$ ).

The schematic in Figure 7c depicts the proposed mechanism by which controlling GO sonication time can tune the amount of drug loaded into and released from the nanocomposite. The drug-loaded GO/PPy nanocomposite is electropolymerized from an aqueous solution containing GO sheets and DEX molecules, creating an opportunity for the drug to adsorb onto the surface of the nanosheets prior to film deposition. With longer sonication treatment, more GO sheets are present in the polymerization suspension as each multilayer GO particle is exfoliated into several s/fGO sheets. Prior to electrodeposition, the GO sheets load some DEX molecules onto their surfaces through physical adsorption and then compete with the remaining free DEX molecules as dopants during the polymerization reaction. When GO undergoes sonication, the nanoparticle size decreases in the z-direction as each multilayered GO exfoliates into multiple s/fGO particles

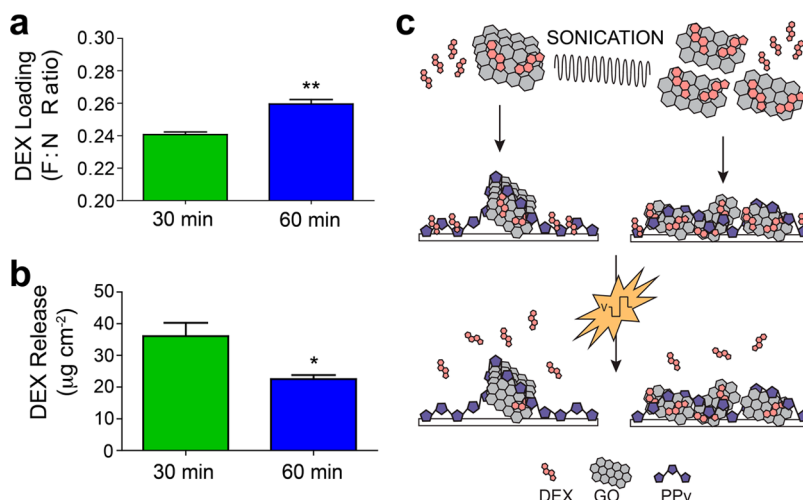


**Figure 7.** Effect of GO sheet sonication on GO/PPy nanocomposite properties. (a) Elemental analysis of GO/PPy-DEX nanocomposite film. The F/N ratio reflects the amount of drug loaded into the film. Longer sonication treatment yields a higher quantity of drug loading (\*\* $p < 0.01$ ;  $n = 3$ ). (b) Amount of DEX released from nanocomposite films in response to 100 voltage pulses ( $-0.5 \text{ V}$  for 5 s, followed by  $0.5 \text{ V}$  for 5 s). Less sonication results in a higher release rate (\* $p < 0.05$ ;  $n = 4$ ). (c) Schematic representation of the effect of GO sheet sonication on nanocomposite properties. With more sonication, the GO nanosheets are separated into more s/fGO particles. The thinner sheets result in a smoother surface morphology and carry more DEX into the film, owing to the larger amount of available surface area for drug molecule adsorption. However, a smaller amount of drug is delivered in response to stimulation, possibly a consequence of the strong adsorption force impeding the electrically driven release. In addition, the sonication treatment alters the morphology of the film, with more sonication resulting in a smoother film surface.

(Figure 6a) and in the  $x$ -/ $y$ -direction as each GO sheet breaks into several smaller sheets (Figure 6b), creating a larger number of smaller particles that would act as more efficient dopant molecules.<sup>33</sup> In addition, as each multilayered GO sheet exfoliates into multiple s/fGO particles, a larger number of reactive nanosheet edges containing negatively charged carboxylic acid groups will be present, leading to more GO nanosheets depositing into the nanocomposite film. Because each GO sheet can carry multiple drug molecules into the film, a larger total amount of DEX can be loaded as a result of increased sonication treatment.

We propose that the strong adsorption of DEX molecules onto the GO sheets is the mechanism behind the slowed drug-release rate. Because more GO nanosheets are likely to be incorporated into the nanocomposite as the amount of sonication time increases, there is likely to be less DEX directly doped into the film. Potentially, the DEX molecules adsorbed onto the surface of the GO nanosheet cannot be released from the film as easily as directly doped DEX molecules because of the strength of the  $\pi$ - $\pi$  interactions, limiting the amount of drug release in response to the same electrical stimulation. Potentially, as the directly doped DEX molecules exit the film upon electrical stimulation, the GO-adsorbed DEX molecules may desorb from the sheets, diffuse through the PPy matrix, and replenish the doping sites. By this mechanism, the release profile of the nanocomposite would be extended. With future work to explore the GO-drug adsorption/desorption phenomenon, the unique properties of the GO/PPy nanocomposite could be

utilized to create a highly tunable release system with the ability to address various dosing needs for a multitude of drug delivery applications.

Along with providing control over drug loading and release, the GO nanosheets create a unique opportunity to alter the morphological characteristics of the nanocomposite film. Sonication had a significant effect on the morphology of the GO/PPy-DEX film (Figure 8). With less GO sonication, the film exhibited globular, cauliflower-like features on the scale of tens of micrometers that are characteristic of PPy films (Supporting Information Figure S2).<sup>24</sup> As the amount of GO sonication increased from 30 to 60 min, the large globular features flattened to create a more uniform surface (Figure 8c). The large features are possibly a result of nucleation sites created by the multilayer GO nanoparticles. As the nanoparticles deposit into the film, they provide a scaffold around which the growing polymer can accumulate. After a longer sonication time, the smaller s/fGO particles distribute more evenly in the film, creating a smoother surface (Figure 7c). At a smaller scale, small sheet-like features became more apparent at the surface of the film, suggesting that more GO sheets are incorporated into the nanocomposite (Figure 8d). At the 60 min sonication time point, the sheet-like features reduced in size to submicrometer dimensions, as would be expected, because increased sonication treatment fractures GO sheets into smaller particles. The ability to subtly alter the nanocomposite surface morphology at different length scales can have important implications for applications in which the film interacts with tissue or cells.

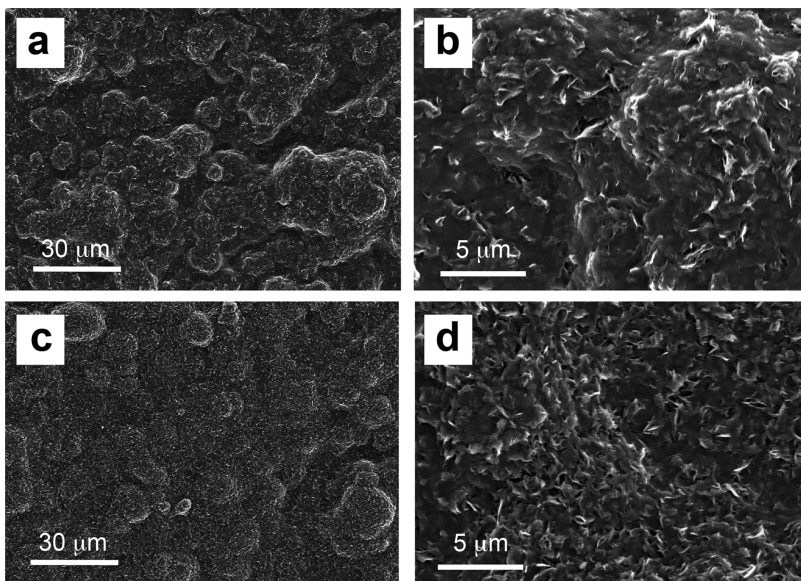


**Figure 8. Effect of GO sonication on GO/PPy film morphology.** SEM images of GO/PPy-DEX films prepared with GO sonicated for (a,b) 30 min and (c,d) 60 min. Longer sonication time results in a smoother surface morphology and the emergence of more sheet-like features at the surface of the film.

Multiple cell types have demonstrated sensitivity toward mechanical and topographical cues in their environment, suggesting that the nanocomposite film morphology may be engineered to act synergistically with electrically controlled drug release to provide additional signals to the targeted cell population.<sup>40–42</sup>

## CONCLUSIONS

The unique properties of GO sheets enable several degrees of customizability to the electrically controlled drug-release platform. By altering the size and thickness of the nanosheets, significant changes can be made to nanocomposite film morphology, drug load, and drug-release properties. As a nanocarrier, GO may enable loading of a variety of biomolecules, not limited to anionic species, into the film. Furthermore, the

GO/PPy nanocomposite film exhibits a linear release profile that persists over several hundred stimulations, indicating that the release platform could be used for long-term drug-release applications that require repeated dosing over time. On-demand controlled drug delivery provides more effective therapies with less toxicity by tuning delivery directly to spatial and temporal requirements for a given application. In addition, controlled delivery may be beneficial in various *in vitro* assays, such as high-throughput drug screening or exploratory cell biology experimentation. As a result of its adjustable properties, stability, and fine control over dosing, the novel GO nanocomposite release platform described here has the potential to advance these drug delivery technologies by enabling tailored drug-release profiles.

## MATERIALS AND METHODS

**Electrochemical Apparatus.** All electrochemical experiments were performed with a Gamry potentiostat, FAS2/femtostat (Gamry Instruments), using a three-electrode setup with glassy carbon working electrodes (3 mm diameter, CH Instruments), a platinum wire counter electrode, and a silver/silver chloride reference electrode (CH Instruments).

**GO Synthesis.** GO was synthesized from graphite powder (SP-1, Bay Carbon Inc., Bay City). A preoxidation step was performed to increase the extent of oxidation of the final product, followed by oxidation by the modified Hummer's method.<sup>43,44</sup> In brief, a solution of 50 mL of H<sub>2</sub>SO<sub>4</sub>, 10 g of K<sub>2</sub>S<sub>2</sub>O<sub>8</sub>, and 10 g of P<sub>2</sub>O<sub>5</sub> was heated to 80 °C. Graphite powder (12 g) was added and reacted for 6 h at 80 °C. The solution was diluted with 2 L of dH<sub>2</sub>O, filtered through a glass filter (pore size: 2.5–4.5 μm), and air-dried overnight. The pretreated graphite (688.5 mg) was added to 23 mL of H<sub>2</sub>SO<sub>4</sub> chilled to 0 °C, and 3 g of KMnO<sub>4</sub> was added while the temperature was controlled below 10 °C. The solution was reacted for 2 h at 35 °C, and then 46 mL of dH<sub>2</sub>O was added while the temperature was controlled

below 50 °C. The solution was reacted for an additional 2 h at 35 °C and then was diluted with 140 mL of dH<sub>2</sub>O. A 2.5 mL volume of H<sub>2</sub>O<sub>2</sub> (30%) was added, and the mixture was allowed to settle overnight. After decanting the supernatant, the GO was washed by ultracentrifugation with 500 mL of HCl, followed by washing with copious dH<sub>2</sub>O until the wash solution reached a neutral pH value. The GO was dialyzed for 4 days and then stored in H<sub>2</sub>O until use.

**Nanocomposite Film Synthesis.** GO/PPy-DEX nanocomposite films were electrochemically synthesized on the glassy carbon electrodes from an aqueous solution containing pyrrole (0.2 M, Sigma-Aldrich), dexamethasone 21-phosphate disodium salt (10 mg mL<sup>-1</sup>, Sigma-Aldrich), and GO nanosheets (5 mg mL<sup>-1</sup>). The GO suspension was ultrasonicated for 30 or 60 min immediately prior to electropolymerization. A constant potential of 0.8 V vs a silver/silver chloride reference electrode was applied until the charge density reached 400 mC cm<sup>-2</sup>. Conventional PPy-DEX films were electrochemically synthesized under the same conditions, with the exclusion of the GO nanosheets from the aqueous polymerization solution.

**Electrochemical Measurements.** Electrochemical impedance spectra of prepared films were collected in PBS, in the frequency range of 1 to 100 kHz, using an alternating current sinusoid of 5 mV. CV analysis was performed in PBS by sweeping the potential from  $-0.9$  to  $0.5$  V at  $100\text{ mV s}^{-1}$ .

**Nanosheet and Film Characterization.** GO nanosheet thickness and size was evaluated with atomic force microscopy (Bruker Dimension V SPM). Nanosheet suspensions were drop-coated on mica surfaces, and the height profile was analyzed in tapping mode. Nanoscope Analysis software (Bruker) was used to calculate the histograms of sheet thicknesses and mean nanosheet diameter after 30 or 60 min sonication treatments. The surface morphology and microstructure of the nanocomposite film were evaluated with scanning electron microscopy (JEOL JSM6510). Film surface chemistry was evaluated with attenuated total reflectance Fourier transform IR (Bruker Vertex 70), and elemental analysis was performed by energy-dispersive X-ray spectroscopy (Oxford INCA EDS).

**Electrically Controlled Drug Release.** For all drug-release experiments, modified electrodes were immersed in PBS and submitted to release stimulation. The PBS solutions containing the released drug were analyzed with UV spectroscopy at a wavelength of  $242\text{ nm}$  to quantify the amount of DEX released. To compare the amount of DEX released from conventional PPY-DEX films and the GO/PPy-DEX nanocomposite, a square wave, biphasic voltage pulse ( $-2\text{ V}$  for  $5\text{ s}$ , followed by  $0\text{ V}$  for  $5\text{ s}$ ) was applied for  $1000$  cycles, and the cumulative amount of DEX release was quantified. To determine total amount of releasable drug from the GO/PPy-DEX nanocomposite, films underwent aggressive voltage pulses ( $-2\text{ V}$  for  $5\text{ s}$ , followed by  $0\text{ V}$  for  $5\text{ s}$ ) until cumulative drug release reached a plateau. The plateau value was considered the total amount of releasable drug contained in the nanocomposite. To evaluate the release profile in response to repeated stimulus application, films were submitted to square wave, biphasic voltage pulses ( $-0.5\text{ V}$  for  $5\text{ s}$ , followed by  $0.5\text{ V}$  for  $5\text{ s}$ ). The amount of drug release was reported as the percentage of total drug release (the plateau value) determined using the aggressive voltage stimulation. The negative phase of the stimulus was varied from  $-2$  to  $-0.25\text{ V}$  to evaluate the stimulus magnitude effect on drug release.

**DEX Loading Capacity Assay.** The amount of DEX loaded on GO sheets was evaluated by incubating DEX ( $100\text{ }\mu\text{M}$ ) with GO ( $0.5\text{ mg mL}^{-1}$ ) in  $\text{H}_2\text{O}$  for  $2\text{ h}$  at room temperature. Prior to incubation with DEX, the GO suspension was sonicated for  $30$  or  $60\text{ min}$ . The mixture was centrifuged for  $30\text{ min}$  at  $14\,000\text{ rpm}$  to pellet the DEX-loaded GO nanosheets, and the supernatant was analyzed with UV spectroscopy at  $242\text{ nm}$  to determine the amount of DEX remaining in solution. The amount of drug loaded was calculated by subtracting the amount of free DEX in the supernatant from the amount of DEX in a sample not incubated with GO.

**Bioactivity Assay.** All animal procedures were approved by the Institutional Animal Care and Use Committee of the University of Pittsburgh. Hippocampal tissue was isolated from E18 Sprague–Dawley rat embryos, treated with a digestion buffer containing  $0.025\%$  trypsin,  $137\text{ mM NaCl}$ ,  $5\text{ mM KCl}$ ,  $7\text{ mM Na}_2\text{HPO}_4$ , and  $25\text{ mM HEPES}$ . For astrocyte cultures, dissociated hippocampal cells were maintained in DMEM supplemented with fetal bovine serum and penicillin/streptomycin, grown to confluence in a culture flask, trypsinized, and seeded on bare glass coverslips at a density of  $15\text{k cells/cm}^2$ . The cultures were incubated for  $1\text{ h}$  at  $37^\circ\text{C}$  to allow cell attachment and then were treated with release solutions from the GO/PPy-DEX films (rDEX) or a prepared DEX solution. The DEX release solutions were obtained by applying an aggressive voltage stimulation paradigm ( $-2\text{ V}$  for  $5\text{ s}$ , followed by  $0\text{ V}$  for  $5\text{ s}$ ,  $1000$  cycles) to the GO/PPy-DEX film. The total amount of DEX in the release solution was quantified using UV spectroscopy, and a volume was added to the culture media to create a concentration of  $1\text{ }\mu\text{M}$  DEX. For neuron cultures, dissociated hippocampal cells were maintained in Neurobasal with B27, GlutaMax, horse serum and penicillin/streptomycin. Glass coverslips were prepared for neuron culture by coating with polyethylenimine (PEI) followed by laminin, and neurons were seeded on the coverslips at a density of  $25\text{k cells/cm}^2$ . To evaluate any toxic byproduct

released from the films, control films without drug underwent the same aggressive electrical stimulation parameters as the drug-loaded films, and the resulting release solutions were added to the neuronal culture at the same volumes as the treatments.

**Immunofluorescence.** After  $2\text{ days}$  (neurons) or  $4\text{ days}$  (astrocytes), the cultures were fixed in  $4\%$  paraformaldehyde for  $30\text{ min}$ . The cells were blocked and permeabilized by immersion in a solution containing  $5\%$  normal goat serum and  $0.2\%$  TritonX. Neuron cultures were immunostained with mouse monoclonal anti- $\beta$ -III-tubulin (1:500, Sigma-Aldrich), and astrocyte cultures were immunostained with polyclonal rabbit antiguial fibrillary acidic protein (GFAP, 1:500, Dako). For both culture types, the samples were incubated in the primary antibody for  $2\text{ h}$ , washed with PBS, incubated in a goat Alexa Fluor 488 (1:1000, Invitrogen) against the appropriate species for  $45\text{ min}$ , washed in PBS, and counterstained for nuclei with Hoechst 33342 (1:1000, Invitrogen). Immunoreactive cells were imaged with a Zeiss Axioskop 2 fluorescent microscopic. Six random  $10\times$  images were collected from each sample ( $n = 4$ ), and mean neuron density, average neurite length, and astrocyte density were quantified.

**Statistical Analysis.** All statistical analyses were done using SPSS software (IBM). Student's *t* tests or one-way analysis of variance (ANOVA), followed by Tukey's post-hoc analysis, were used to compare experimental groups. All data are presented as mean ( $\pm\text{SEM}$ ).

**Conflict of Interest:** The authors declare no competing financial interest.

**Acknowledgment.** This research was supported by the National Science Foundation Grants 0748001, ERC-0812348, and DGE-0549352 and National Institutes of Health R01NS062019. C.L.W. acknowledges the University of Pittsburgh Provost's Development Fund. X.L. acknowledges the support of the Taishan Scholar Program of Shandong Province, China. The authors would like to thank C. Urbanic for her valuable assistance in editing the manuscript.

**Supporting Information Available:** Fourier transform IR spectra and additional SEM images. This material is available free of charge via the Internet at <http://pubs.acs.org>.

## REFERENCES AND NOTES

- LaVan, D. A.; McGuire, T.; Langer, R. Small-Scale Systems for *In Vivo* Drug Delivery. *Nat. Biotechnol.* **2003**, *21*, 1184–1191.
- Staples, M. Microchips and Controlled-Release Drug Reservoirs. *Wiley Interdiscip. Rev.: Nanomed. Nanobiotechnol.* **2010**, *2*, 400–417.
- Timko, B. P.; Kohane, D. S. Materials to Clinical Devices: Technologies for Remotely Triggered Drug Delivery. *Clin. Ther.* **2012**, *34*, S25–S35.
- Mura, S.; Nicolas, J.; Couvreur, P. Stimuli-Responsive Nanocarriers for Drug Delivery. *Nat. Mater.* **2013**, *12*, 991–1003.
- Timko, B. P.; Dvir, T.; Kohane, D. S. Remotely Triggerable Drug Delivery Systems. *Adv. Mater.* **2010**, *22*, 4925–4943.
- Balmert, S. C.; Little, S. R. Biomimetic Delivery with Micro- and Nanoparticles. *Adv. Mater.* **2012**, *24*, 3757–3778.
- Zhang, L.; Gu, F. X.; Chan, J. M.; Wang, A. Z.; Langer, R. S.; Farokhzad, O. C. Nanoparticles in Medicine: Therapeutic Applications and Developments. *Clin. Pharm. Ther.* **2008**, *83*, 761–769.
- Bianco, A.; Kostarelos, K.; Prato, M. Applications of Carbon Nanotubes in Drug Delivery. *Curr. Opin. Chem. Biol.* **2005**, *9*, 674–679.
- Yang, K.; Feng, L.; Shi, X.; Liu, Z. Nano-graphene in Biomedicine: Theranostic Applications. *Chem. Soc. Rev.* **2013**, *42*, 530–547.
- Dreyer, D. R.; Park, S.; Bielawski, C. W.; Ruoff, R. S. The Chemistry of Graphene Oxide. *Chem. Soc. Rev.* **2010**, *39*, 228–240.
- Luo, X.; Weaver, C. L.; Tan, S.; Cui, X. T. Pure Graphene Oxide Doped Conducting Polymer Nanocomposite for Bio-interfacing. *J. Mater. Chem. B* **2013**, *1*, 1340–1348.

12. Sanchez, V. C.; Jachak, A.; Hurt, R. H.; Kane, A. B. Biological Interactions of Graphene-Family Nanomaterials: An Interdisciplinary Review. *Chem. Res. Toxicol.* **2012**, *25*, 15–34.
13. Wang, Y.; Li, Z.; Wang, J.; Li, J.; Lin, Y. Graphene and Graphene Oxide: Biofunctionalization and Applications in Biotechnology. *Trends Biotechnol.* **2011**, *29*, 205–212.
14. Li, M.; Yang, X. J.; Ren, J. S.; Qu, K. G.; Qu, X. G. Using Graphene Oxide High Near-Infrared Absorbance for Photo-thermal Treatment of Alzheimer's Disease. *Adv. Mater.* **2012**, *24*, 1722–1728.
15. Tao, Y.; Lin, Y. H.; Huang, Z. Z.; Ren, J. S.; Qu, X. G. Incorporating Graphene Oxide and Gold Nanoclusters: A Synergistic Catalyst with Surprisingly High Peroxidase-like Activity over a Broad pH Range and Its Application for Cancer Cell Detection. *Adv. Mater.* **2013**, *25*, 2594–2599.
16. Sun, X. M.; Liu, Z.; Welsher, K.; Robinson, J. T.; Goodwin, A.; Zaric, S.; Dai, H. J. Nano-Graphene Oxide for Cellular Imaging and Drug Delivery. *Nano Res.* **2008**, *1*, 203–212.
17. Yang, X. Y.; Zhang, X. Y.; Liu, Z. F.; Ma, Y. F.; Huang, Y.; Chen, Y. High-Efficiency Loading and Controlled Release of Doxorubicin Hydrochloride on Graphene Oxide. *J. Phys. Chem. C* **2008**, *112*, 17554–17558.
18. Depan, D.; Shah, J.; Misra, R. D. K. Controlled Release of Drug from Folate-Decorated and Graphene Mediated Drug Delivery System: Synthesis, Loading Efficiency, and Drug Release Response. *Mater. Sci. Eng., C* **2011**, *31*, 1305–1312.
19. Ma, X. X.; Tao, H. Q.; Yang, K.; Feng, L. Z.; Cheng, L.; Shi, X. Z.; Li, Y. G.; Guo, L.; Liu, Z. A Functionalized Graphene Oxide–Iron Oxide Nanocomposite for Magnetically Targeted Drug Delivery, Photothermal Therapy, and Magnetic Resonance Imaging. *Nano Res.* **2012**, *5*, 199–212.
20. Yang, X. Y.; Wang, Y. S.; Huang, X.; Ma, Y. F.; Huang, Y.; Yang, R. C.; Duan, H. Q.; Chen, Y. S. Multi-functionalized Graphene Oxide Based Anticancer Drug-Carrier with Dual-Targeting Function and pH-Sensitivity. *J. Mater. Chem.* **2011**, *21*, 3448–3454.
21. Yang, X. Y.; Zhang, X. Y.; Ma, Y. F.; Huang, Y.; Wang, Y. S.; Chen, Y. S. Superparamagnetic Graphene Oxide–Fe<sub>3</sub>O<sub>4</sub> Nanoparticles Hybrid for Controlled Targeted Drug Carriers. *J. Mater. Chem.* **2009**, *19*, 2710–2714.
22. Zhang, L. M.; Xia, J. G.; Zhao, Q. H.; Liu, L. W.; Zhang, Z. J. Functional Graphene Oxide as a Nanocarrier for Controlled Loading and Targeted Delivery of Mixed Anticancer Drugs. *Small* **2010**, *6*, 537–544.
23. Liu, H. W.; Hu, S. H.; Chen, Y. W.; Chen, S. Y. Characterization and Drug Release Behavior of Highly Responsive Chip-like Electrically Modulated Reduced Graphene Oxide–Poly(vinyl alcohol) Membranes. *J. Mater. Chem.* **2012**, *22*, 17311–17320.
24. Svirskis, D.; Travas-Sejdic, J.; Rodgers, A.; Garg, S. Electro-chemically Controlled Drug Delivery Based on Intrinsically Conducting Polymers. *J. Controlled Release* **2010**, *146*, 6–15.
25. Kontturi, K.; Pentti, P.; Sundholm, G. Polypyrrole as a Model Membrane for Drug Delivery. *J. Electroanal. Chem.* **1998**, *453*, 231–238.
26. Thompson, B. C.; Moulton, S. E.; Ding, J.; Richardson, R.; Cameron, A.; O'Leary, S.; Wallage, G. G.; Clark, G. M. Optimising the Incorporation and Release of a Neurotrophic Factor Using Conducting Polypyrrole. *J. Controlled Release* **2006**, *116*, 285–294.
27. Luo, X.; Cui, X. T. Electrochemically Controlled Release Based on Nanoporous Conducting Polymers. *Electrochim. Commun.* **2009**, *11*, 402–404.
28. Osterholm, A.; Lindfors, T.; Kauppila, J.; Damlin, P.; Kvamstrom, C. Electrochemical Incorporation of Graphene Oxide into Conducting Polymer Films. *Electrochim. Acta* **2012**, *83*, 463–470.
29. Zhu, C. Z.; Zhai, J. F.; Wen, D.; Dong, S. J. Graphene Oxide/Polypyrrole Nanocomposites: One-Step Electrochemical Doping, Coating and Synergistic Effect for Energy Storage. *J. Mater. Chem.* **2012**, *22*, 6300–6306.
30. Si, P.; Chen, H. L.; Kannan, P.; Kim, D. H. Selective and Sensitive Determination of Dopamine by Composites of Polypyrrole and Graphene Modified Electrodes. *Analyst* **2011**, *136*, 5134–5138.
31. Si, W. M.; Lei, W.; Zhang, Y. H.; Xia, M. Z.; Wang, F. Y.; Hao, Q. L. Electrodeposition of Graphene Oxide Doped Poly(3,4-ethylenedioxythiophene) Film and Its Electrochemical Sensing of Catechol and Hydroquinone. *Electrochim. Acta* **2012**, *85*, 295–301.
32. Lee, W. C.; Lim, C. H.; Shi, H.; Tang, L. A.; Wang, Y.; Lim, C. T.; Loh, K. P. Origin of Enhanced Stem Cell Growth and Differentiation on Graphene and Graphene Oxide. *ACS Nano* **2011**, *5*, 7334–7341.
33. Vernitskaya, T. V.; Efimov, O. N. Polypyrrole: A Conducting Polymer (Synthesis, Properties, and Applications). *Russ. Chem. Rev.* **1997**, *66*, 489–505.
34. Miller, L. L.; Zinger, B.; Zhou, Q. X. Electrically Controlled Release of Hexacyanoferrate(4-) from Polypyrrole. *J. Am. Chem. Soc.* **1987**, *109*, 2267–2272.
35. Unemura, K.; Kume, T.; Kondo, M.; Maeda, Y.; Izumi, Y.; Akaike, A. Glucocorticoids Decrease Astrocyte Numbers by Reducing Glucocorticoid Receptor Expression *In Vitro* and *In Vivo*. *J. Pharmacol. Sci.* **2012**, *119*, 30–39.
36. Bianco, A. Graphene: Safe or Toxic? The Two Faces of the Medal. *Angew. Chem., Int. Ed.* **2013**, *52*, 4986–4997.
37. Sharifi, S.; Behzadi, S.; Laurent, S.; Forrest, M. L.; Stroeve, P.; Mahmoudi, M. Toxicity of Nanomaterials. *Chem. Soc. Rev.* **2012**, *41*, 2323–2343.
38. Russier, J.; Treossi, E.; Scarsi, A.; Perrozzi, F.; Dumortier, H.; Ottaviano, L.; Meneghetti, M.; Palermo, V.; Bianco, A. Evidencing the Mask Effect of Graphene Oxide: A Comparative Study on Primary Human and Murine Phagocytic Cells. *Nanoscale* **2013**, *5*, 11234–11247.
39. Luo, J.; Kim, J.; Huang, J. Material Processing of Chemically Modified Graphene: Some Challenges and Solutions. *Acc. Chem. Res.* **2013**, *46*, 2225–2234.
40. Kolind, K.; Leong, K. W.; Besenbacher, F.; Foss, M. Guidance of Stem Cell Fate on 2D Patterned Surfaces. *Biomaterials* **2012**, *33*, 6626–6633.
41. Yim, E. K.; Leong, K. W. Significance of Synthetic Nanostructures in Dictating Cellular Response. *Nanomedicine* **2005**, *1*, 10–21.
42. Zhang, B.; Xiao, Y.; Hsieh, A.; Thavandiran, N.; Radisic, M. Micro- and Nanotechnology in Cardiovascular Tissue Engineering. *Nanotechnology* **2011**, *22*, 494003.
43. Hummers, W. S.; Offeman, R. E. Preparation of Graphitic Oxide. *J. Am. Chem. Soc.* **1958**, *80*, 1339.
44. Li, Y.; Wu, Y. Coassembly of Graphene Oxide and Nanowires for Large-Area Nanowire Alignment. *J. Am. Chem. Soc.* **2009**, *131*, 5851–5857.